

Analysis of the techniques for assessing the features of blast-induced fragmentation in an open pit quarry

Original

Analysis of the techniques for assessing the features of blast-induced fragmentation in an open pit quarry / Cardu, M.; Calzamiglia, A.. - ELETTRONICO. - (2021). (Intervento presentato al convegno EUROCK 2021 - Mechanics and Rock Engineering, from Theory to Practice tenutosi a Torino nel 20-25 September 2021) [10.1088/1755-1315/833/1/012121].

Availability:

This version is available at: 11583/2929189 since: 2021-10-05T15:40:57Z

Publisher:

IOP Conference Series: Earth and Environmental Science

Published

DOI:10.1088/1755-1315/833/1/012121

Terms of use:

openAccess

This article is made available under terms and conditions as specified in the corresponding bibliographic description in the repository

Publisher copyright

(Article begins on next page)

PAPER • OPEN ACCESS

Analysis of the techniques for assessing the features of blast-induced fragmentation in an open pit quarry

To cite this article: M Cardu and A Calzamiglia 2021 *IOP Conf. Ser.: Earth Environ. Sci.* **833** 012121

View the [article online](#) for updates and enhancements.



ECS **240th ECS Meeting**
Digital Meeting, Oct 10-14, 2021

We are going fully digital!

Attendees register for free!

REGISTER NOW

Analysis of the techniques for assessing the features of blast-induced fragmentation in an open pit quarry

M Cardu ^{1,2}, A Calzamiglia ¹

¹. DIATI Politecnico di Torino, Italy

². IGG-CNR Torino, Italy

marilena.cardu@polito.it

Abstract. The paper deals with the study of empirical models for the analysis of blasts-induced fragmentation. To verify the reliability of the method, the results obtained a priori through the application of the models are compared with the analyses of muck piles photos taken from a series of blasts in an open pit quarry, thanks to the Split-desktop software (*Split Engineering, LLC*, Tucson, USA). The study of the particle size distribution is very important when sizing an excavation site, as the average size of the pile must be compatible with the equipment used for clearing and conveyance, and with the first phase of the processing plant, i.e. primary crushing. After a description of the excavation technique in use at the quarry site, its main characteristics are outlined. The parameters used to create the empirical models refer to the geomechanical characteristics of the rock, the geometry of the blasts, the characteristics of the explosive and its interaction with the rock mass, paying attention to the correlation between initiation timing and induced fragmentation. A detailed description of some empirical models together with the Split-desktop software were therefore provided. Thanks to both data and photos of the muck-piles from the exploitation at the quarry, the particle size curves resulting from each model were compared with those obtained from the software. This allowed to validate the empirical method in a preliminary design phase.

1. Introduction

The production cycle of an exploitation site generally develops in two phases, that of excavation and that of processing. The excavation technique depends on both the type of deposit and the geomechanical characteristics of the exploited material. In this case, the drill and blast technique will be analysed for an open pit quarry. As known, this technique involves carrying out a series of cyclical operations, consisting of: evaluation of the geometry of the blast, choice of explosives and initiation systems, charging and initiation, scaling, loading, hauling and dumping. Based on the different phases of the cycle, there are many factors that influence and are influenced by the size of the blasted material [1]. Particularly, the grain size distribution and its maximum size D_{max} is important, as it represents the maximum size that the opening of the crusher jaws can accept. Therefore, the desired fragmentation is a key parameter in the design of a blast [2 – 3]; it is influenced by the drilling diameter, the blasting pattern, the type and the amount of charge used [4]. To study the fragmentation induced by a blast, the geomechanical properties of the rock mass and its response to explosives have to be considered: as a first approximation, the impedance of the "rock-explosive" pair is a parameter that allows an a priori estimation of the result of a blast in a given rock mass [5].



Some small-scale laboratory tests were performed to evaluate the effect of timing on fragmentation [3]; these tests were developed on small size limestone blocks, around 60 cm x 40 cm x 25 cm, by using different delay times and different patterns. The results showed that the average size decreases dramatically at short delay times (less than 0.1 ms), while it appears to be constant between 0.2 and 1 ms, and increases slightly for longer delays. The research also found that timing mainly affects grains with larger sizes (x_{80}), whereas finer grains (x_{20}) behave almost the same for delays greater than 0.1 ms. The delay time also affects the fragmentation uniformity and it can be stated that it is greater for delay times of about 0.2 ms than for longer delay times (0.7 ms).

The study of the grain size distribution from a blast can be carried out thanks to direct or indirect methods. The most common direct method is by sieving: the test is conducted by placing a series of sieves with progressively smaller mesh sizes on top of each other and passing the sample through the stacked sieve "tower". Therefore, the particles are distributed as they are retained by the different sieves. The graphic result is the grain size distribution curve.

Among the indirect methods, the following can be quoted: observational method; empirical methods, and image analysis.

The empirical models are based on the knowledge of the type of explosive, on the delays used, on the geometry of the blast and the type of rock to be exploited. The most commonly used are: Kuz-Ram model [6]; Crush-zone model [7], KCO Model [8, 9], SveDeFo Model, [1], [10, 11], Kou-Rustan [12], Chung-Katsabanis [13] and xP-frag [14]. The empirical models return the percentage of passing on the basis of the grains size, apart from xP-frag model, which assumes a given percentage of passing and, on the basis of a series of parameters, quantifies its size at that percentage.

2. Empirical models for the definition of a grain size distribution curve

2.1. The Kuz-Ram model

Some The model was first developed by Kuznetov [6] and, following numerous rearrangements by other authors, [15] rewrote the equation as follows:

$$\bar{X} = A \cdot q^{\frac{4}{3}} \cdot Q^{\frac{1}{6}} \quad [m] \quad (1)$$

where: \bar{X} is the average size distribution of the grains, A is a coefficient linked to the rock type, q is the powder factor, Q is the charge/hole.

Since the (1) does not consider the type of explosive, Kuznetov [6] modified the equation by making q explicit with reference to the TNT equivalent.

Later on, the formula was reinterpreted by numerous authors [15], [16], [8], [17], [18], who stated several empirical models to determine the average size of the muck-pile after blasting. Cunningham [15] rewrote the equation (1) as follows:

$$x_{50} = A \cdot q^{-0.8} \cdot Q^{\frac{1}{6}} \cdot \left[\frac{E}{115} \right]^{\frac{19}{30}} \quad [m] \quad (2)$$

where: x_{50} [m] is the average grain size, Q [kg] is the charge/hole, E is the energy of the explosive with respect to ANFO, also known as RWS (Relative Weight Strength), 115 is the RWS of the TNT. An important change was made in terms of the A coefficient calculation: since it is related to the type and quality of the rock mass, Cunningham expressed it as a function of the discontinuities, density and hardness of the rock:

$$A = 0,06 \cdot (RMD + RDI + HF) \quad (3)$$

where RDI (Rock Density Influence), is related to the density of the rock, according to the equation:

$$DI = \left(25 \cdot \frac{\rho}{1000} \right) - 50 \quad \left[\frac{t}{m^3} \right] \quad (4)$$

HF (Hardness Factor) can assume two values depending on the elastic modulus of the rock: $HF=E/3$, if $E<50$ GPa; $HF=\sigma_c/5$, if $E>50$ GPa.

The Rock Mass Description RDI takes into account both spacing and orientation of the discontinuities: it is = 10 for densely fracturing rocks, and 50 for massive rocks; if the dip angle of the discontinuities is greater than 30° , it is = JF, where $JF=JPS+JPA$. JPS (Joint Plane Spacing) can vary depending on the spacing between the discontinuities: it is worth = 10 for spacing <0.1 m, = 20 for 0.1 m $<$ spacing $<$ oversize, and = 50 for spacing $>$ oversize; JPA (Joint Plane Angle) can vary depending on the dip direction of the joints, and it is = 20 for dip out of face, = 30 for normal to face strike, = 40 for dip into face. Once the average size of the fragments from the blast has been evaluated, the passing % is calculated referring to this size. The Rosin-Rammler distribution is therefore applied:

$$R_x = \exp \left[-0,693 \cdot \left(\frac{x}{x_{50}} \right)^n \right] \quad (5)$$

where: R_x is the amount of retained material, x [mm] is the size of the grains, n is the uniformity index, and x_{50} [mm] is the average size of passing.

To calculate the passing %, eq. (5) can be used, with some changes:

$$P(x) = 1 - \exp \left(- \left(\ln(2) \cdot \left(\frac{x}{x_{50}} \right)^n \right) \right) \quad (6)$$

Once the rock type is known and the explosive is chosen, the geometry of the blast can be assessed. There are three factors that influence both the x_{50} and the uniformity index: the burden, the spacing and the drilling diameter. It follows that: if the burden increases, x_{50} also increases, while n decreases; when the spacing increases, both n and x_{50} increase accordingly; the drilling diameter, being proportional to n and inversely proportional to the square of x_{50} , involves an increase of the passing % [19].

2.2. The Crush-zone model

The crush-zone model [20 – 23], [2], [24], [25] assumes that the fines produced by a blast are due to both compression and shear failure, and that the coarse fragments are obtained due to the tensile failure. The crush-zone can be studied by knowing its radius r_c [mm], the volume V_c that a blast-hole can crush and the fraction of fines F_c ; different formulas can be used to calculate r_c :

Djordjevic et al. [21]: the radius of the crush-zone is estimated by equating the stress produced by a uniform distribution of the charge with the uniaxial compressive strength of the rock;

$$r_c = r_0 \sqrt{\frac{(\rho_e \cdot D^2)}{8 \cdot \sigma_c}} \quad [\text{mm}] \quad (7)$$

where: r_0 [mm] is the hole diameter, D [m/s] is the detonation velocity, ρ_e $\left[\frac{\text{kg}}{\text{m}^3} \right]$ is the charge density, σ_c [Pa] is the uniaxial compressive strength of the rock.

Szuladzinski [24]: the rock is considered as an elastic body with a compressive capacity and strength:

$$r_c = \sqrt{\frac{2 \cdot r_0^2 \cdot \rho_e \cdot Q_{ef}}{F'_c}} \quad [\text{mm}] \quad (8)$$

where: r_0 [mm] is the hole radius, ρ_e $\left[\frac{\text{g}}{\text{mm}^3} \right]$ is the charge density, Q_{ef} $\left[\frac{\text{N} \cdot \text{mm}}{\text{g}} \right]$ is the explosive specific energy, F'_c [MPa] is the confined dynamic compressive strength of the rock mass. Usually, $F'_c = 8 \cdot \sigma_c$.

Djordjevic [25]: the formula is based on Griffith's failure criterion:

$$r_c = \frac{r_0}{\sqrt{\frac{24T}{P_b}}} \quad [\text{mm}] \quad (9)$$

where: T [Pa] is the tensile rock strength, $P_b = \frac{\rho_c \cdot D^2}{8}$ [Pa] is the detonation pressure.

Once the radius of the crushing zone has been calculated, the volume of fractured rock per hole V_c has to be quantified:

$$V_c = \pi \cdot (r_c^2 - r_0^2) \cdot (H - l_s) \quad [\text{m}^3] \quad (10)$$

where: r_c [m] is the radius of the crushing zone, r_0 [m] is the hole radius, H [m] is the bench height, l_s [m] is the stemming length.

Once the volume V_c is known, the fraction of fines F_c can be calculated through the equation:

$$F_c = \frac{V_c}{B_h \cdot S \cdot H} \quad [-] \quad (11)$$

where: $B_h = \frac{B}{\cos i}$ [m], i.e. the burden as a function of the hole deviation i [rad], S [m] being the spacing, H [m] the bench height.

2.3. The KCO Model

The model is named after Kuznetsov, Cunningham and Ouchterlony and is based on the Swebrec function [9]. Basically, it employs a new distribution function, which replaces that of Rosin Rammler (6):

$$P(x) = \frac{1}{1 + \left(\frac{\ln\left(\frac{x_{\max}}{x}\right)}{\ln\left(\frac{x_{\max}}{x_{50}}\right)} \right)^b} \quad (12)$$

where: $x_{\max} = \min(B, S, l_b)$ [cm], x_{50} [cm] is the average size of the fragments, b is the wave parameter of the curve and is given by the equation:

$$b = 0,5 \cdot x_{50}^{0,25} \cdot \ln\left(\frac{x_{\max}}{x_{50}}\right) \quad (13)$$

This model adapts very well to fragments size $0.5 < x < 500$ [mm] but it is limited at the top by x_{\max} .

2.4. The SveDeFo Model

The Swedish Detonics Research Foundation [10] has developed a model that takes into account the type of rock mass and the geometry of the blast. Compared to the previous models, x_{50} is modified as follows:

$$x_{50} = \frac{1}{6,99} \cdot \left(B^2 \cdot \sqrt{\frac{1,25}{S}} \right)^{0,29} \cdot \left(\frac{c}{s \cdot q} \right)^{1,35} \quad (14)$$

where: x_{50} [m] is the average size of the fragments, B [m] the burden, S [m] the spacing, c [kg/m^3] a constant depending on the rock, which is proportional to the Powder Factor, q [kg/m^3] the Powder Factor, s the force that takes into account the heat of explosion and the volume of gaseous products; for ANFO, $s = 0.84$.

x_{50} is strictly related to the ratio S/B , and increases the more S is greater than B . Another difference compared to the previous models can be found in the grain distribution function, as the uniformity index (n) changes, assuming a constant value:

$$P(x)=1-\exp\left(-0,76\cdot\left(\frac{x}{x_{50}}\right)^{1,35}\right) \quad (15)$$

2.5. The Kou-Rustan Model

It is an extension of SveDeFo, and the most influential parameters are H (bench height), B (burden) and S (spacing). This method was conceived for small-scale blasts, and it is expressed as:

$$x_{50}=\frac{0,01}{B^{0,8}}\cdot\frac{(\rho_r\cdot c_p)^{0,6}\cdot(B\cdot S)^{0,5}}{\left(\frac{L_{tot}}{H}\right)^{0,7}\cdot D^{0,4}\cdot q} \quad [\text{mm}] \quad (16)$$

where: ρ_r [kg/m³] is the rock density, c_p [m/s] the P-waves velocity, L_{tot} [m] the total charged length, D [m] the detonation velocity, q [kg/m³] the Powder Factor.

In this case, the rock is characterized by c_p and ρ_r . The model does not suggest a formula for the percentage of passing: however, the Rosin Rammler distribution can be applied:

$$P(x)=1-\exp\left(-\left(\ln(2)\cdot\left(\frac{x}{x_{50}}\right)^n\right)\right) \quad (17)$$

2.6. The Chung-Katsabanis Model

This model proposes the Rosin Rammler distribution modified according to the Kuz-Ram model, by varying the uniformity index formula, as follows:

$$n=\frac{0,842}{\ln(x_{80})-\ln(x_{50})}=\frac{\ln\left(\frac{\ln 5}{\ln 2}\right)}{\frac{\ln x_{80}}{\ln x_{50}}} \quad (18)$$

x_{50} and x_{80} can be calculated thanks to the following equations, from Kuznetsov's eq. (2):

$$x_{50}=A\cdot Q_e^{-1,193}\cdot B^{2,461}\cdot\left(\frac{S}{B}\right)^{1,254}\cdot H^{1,266} \quad (19)$$

$$x_{80}=3A\cdot Q_e^{-1,073}\cdot B^{2,43}\cdot\left(\frac{S}{B}\right)^{1,013}\cdot H^{1,111} \quad (20)$$

The exponents of B, H and S are low and therefore these parameters can be negligible. As for x_{50} , the blasting pattern can be neglected: therefore, the average size of the grains only depends on the specific charge. The advantage of this model is that fewer parameters are required to calculate x_{50} and x_{80} . However, under a certain size of the fragments, the model is no longer reliable ($x\cong 50$ mm).

2.7. The xP-Frag Model

The formula for calculating the average size of passing is given by the equation:

$$x_p=L_c\cdot k\cdot(J_s+J_0)\cdot k_2^h\cdot\left(\frac{\sigma}{q_e}\right)^\kappa\cdot\frac{1}{L_c^{\lambda\kappa}}\cdot f_t(\Pi_t) \quad (21)$$

where: $L_c=\sqrt{HS}$ [m] is the characteristic hole length, k, h, κ and λ are experimental coefficients, $J_s=\min\left(\frac{s_j}{B}, a_s\right)$ [-] is a factor referring to the joints spacing, s_j [m] is the spacing among the discontinuities, $k_2=\frac{B}{\sqrt{HS}\cdot\cos\theta}$ [-] is the shape factor, $\sigma=(\sigma_c^2)/2E$ [MPa] is the rock-mass strength, $J_0=a_0\cdot j_0$ [-] is linked to the joints orientation, j_0 [-] can vary between 0,25 and 1, q [kg/m³] is the Powder Factor and e [MJ/kg] is the specific energy of the explosive, whereas $f_t(\Pi_t)$ is the exponential of the function Π_t :

$$f_t(\Pi_t) = \delta_1 + (1 - \delta_1 - \delta_2 \cdot \Pi_t) \cdot \exp(-\delta_3 \cdot \Pi_t) \quad (22)$$

Π_t [-] is a timing factor expressed by equation (23); it indicates the blasting pattern geometry as a function of the drilling diameter (represented by the characteristic length L_t) with respect to the distance travelled by the longitudinal waves (P waves) during a delay interval:

$$\Pi_t = (c_p \cdot \Delta t) / L_t \quad (23)$$

where: c_p [m/s] is the P-waves velocity, Δt [s] is the delay among the blast-holes, $L_t = S$ [m] is the spacing.

Once the above parameters have been calculated, the model is developed in order to relate the passing percentage and the grain size distribution [14], [19].

2.8. Comparison among the empirical models

All models are based on the type of rock, explosive, blast geometry and initiation sequence. To take into account the rock mass characteristics, eq. (3) can be used, as well as the rock density (ρ), the P-waves velocity, the orientation of the discontinuities or the uniaxial compressive strength.

The explosives can be described referring to the Powder Factor, combined with different parameters such as: θ (equivalent TNT charge), E (explosive energy with respect to ANFO), D (detonation velocity) and ρ_e (density), s (relative strength, taking into account the heat of explosion and the volume of gases).

As for the blasting pattern, the models refer to the holes' diameter (d), burden (B), spacing (S), bench height (H), and sub-drilling (J); the firing sequence can be set according to the delay of each group of blast-holes (ΔT) or to the delay accuracy (R_s).

3. Image Analysis Method

The software used in the case under study is Split-desktop. It allows evaluating the size of the grains from photographs of the muck-pile from a blast. The photograph must be of high quality and not modified, in order to allow the operator to isolate the individual grains. Furthermore, the presence of at least one (better two) dimensional reference is essential, and there must be no distortion. Finally, the light in the image has to be uniform, not to lose details due to the flash or to the presence of dark areas. Then, the photos can be processed [26].

First, it's necessary to set the scale of the photo, which can be done by entering the size of the chosen reference. In the case under study, a € 0.50 coin was used, by entering the size of the diameter $\phi = 24.25$ mm. Then, the fine cut off must be defined, which depends on the type of rock and the size of the grains. The choice of the fine cut off must also be made on the basis of the capacity/possibility of isolating the finest grains. The image has then to be worked manually, dividing the grains that seem assembled after using the fine cut off and joining, instead, the separate ones. Finally, different dimensions are set to create the grain size distribution curve.

The data used for the application of the empirical models were drawn from the results of some blasts carried out at a limestone quarry located in northern Italy. An example of application of the Split-desktop software is provided with reference to figure 1.

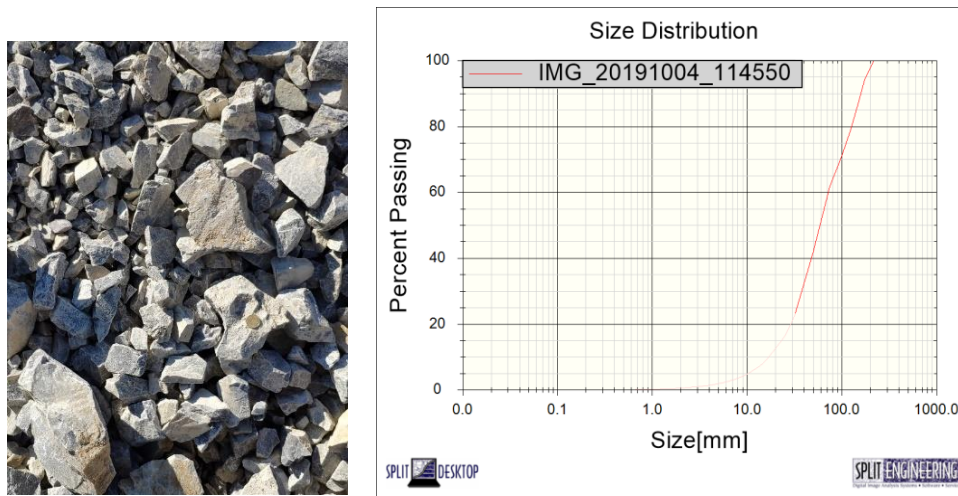


Figure 1. Left: Detail of the muck-pile obtained from a blast in the quarry. A 50 cent coin was used as a reference for scaling the photograph. Right: Grain size distribution referred to the picture; as it's noticeable, the curve is reliable up to a lower limit defined by the fines cut off which, in this case, was set at 32.5 mm. Moreover, the maximum size of fragments found by Split-desktop is 219.5 mm.

The particle size distributions obtained from Split-desktop were compared with those achieved by the application of empirical models. By way of example, the image shown in Figure 1 is considered, since it returns a maximum grain size greater than the others, allowing a better comparison with the empirical models.

3.1. Development of empirical models

Starting from data related to the blast geometry, the characteristics of the rock mass and type and amount of charge used, all the factors necessary to develop the models were calculated.

The exploitation of the quarry takes place on benches with $H = 15$ m, $B = 2$ m and $S = 3$ m. The holes are drilled by a rotary-percussion top hammer with a diameter $d = 101$ mm and inclination $\alpha = 70^\circ$. The deviation of the holes W is on average 0.25 m, the stemming length l_s is 5 m, the sub-drilling J is 1 m, and the deviation angle of the hole i is assumed to be 12° , but it can vary according to the skills of the operator.

As for the characteristics of the rock mass, the useful data for the development of the models are: the density of the rock ρ_r (2710 kg/m^3), the compressive strength σ_c (100 MPa) the elastic modulus E (45 GPa) and the speed of the p-waves c_p (5000 m/s). Furthermore, it was necessary to calculate the factor A (4,965) through the equation (3); therefore, RMD (50), JPS (20), JPA (30) JF (50), RDI (17,8) and HF (15) were assumed.

The explosive used at the quarry is a cartridge ANFO, with specific energy $Q_v = 3,25 \text{ MJ/kg}$, density $\rho_e = 700\text{-}735 \text{ kg/m}^3$, detonation pressure $P = 4060 \text{ MPa}$, volume of gaseous products $V_g = 976 \text{ l/kg}$; detonation velocity $D = 2900 \text{ m/s}$.

On the basis of the data quoted above, empirical models have been developed, whose grain size distribution curves are shown in Figure 2.

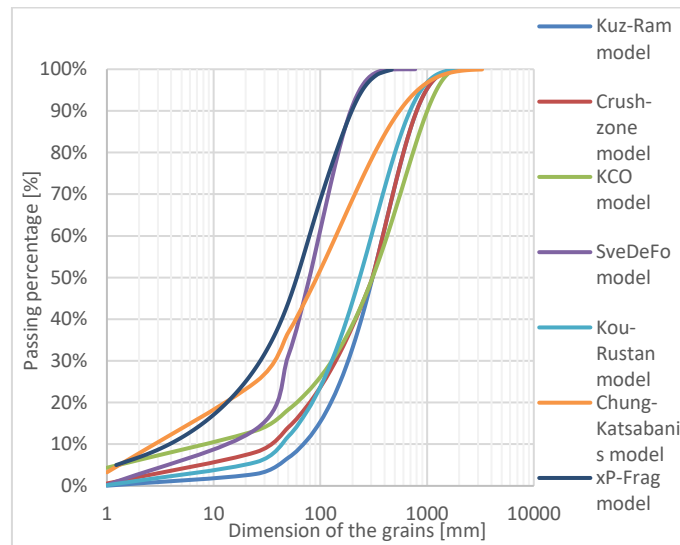


Figure 2. Comparison between the grain size distribution curves obtained by empirical models.

As it can be noticed, the trend of the curves is similar, although the grain size sometimes exceeds that obtained by the photographs. For more detail, graphical comparisons were made between each of the empirical models and the distribution shown in Figure 1: they were limited to the size range between 1 mm and 225 mm, where 1 mm is the minimum limit imposed by the reliability of the empirical models and 225 mm is the maximum size obtained by Split-desktop. By considering the same size, the difference between the curves in Figure 3 is noticeable. The Kuz-Ram model refers to a maximum grain size of about 2000 mm, whereas that of the reference photo is 220 mm but, not taking into account the size of the fragments, the trend of the curves is almost the same. The Crush-zone model behaves similarly to the Kuz-Ram for grains bigger than $x_{50} = 208$ mm.

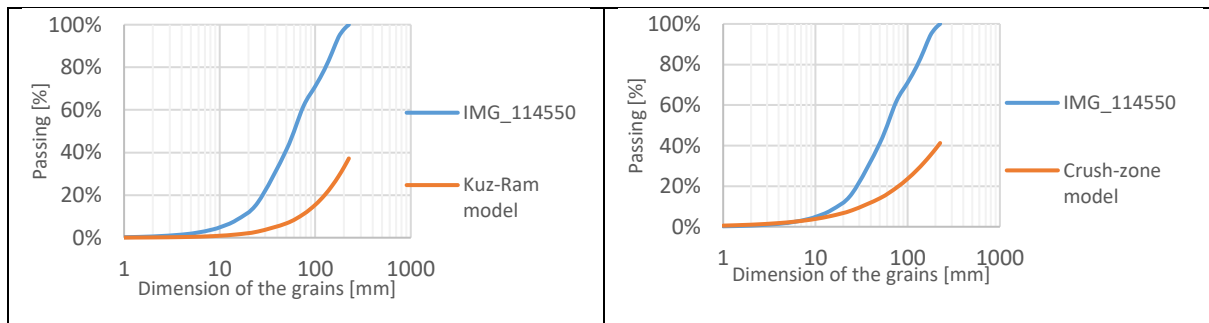


Figure 3. Comparison between the particle size distributions obtained with Split Desktop and those from Kuz-Ram and Crush-zone models.

The trend of KCO (Figure 4) is visibly different, due to the different formulation of the distribution function; then, this model is not recommended for describing the particle size distribution resulting from blasts such as the one analysed. The Kou-Rustan model (Figure 4) behaves similarly to the Kuz-Ram and Crush-zone models. Unlike the latter, however, x_{50} is smaller, being calculated according to another principle. This difference means that the passing percentage, the grain size being the same, is higher, getting closer to the values obtained by the software, showing that the Kou-Rustan can be valid for the description of the muck-pile.

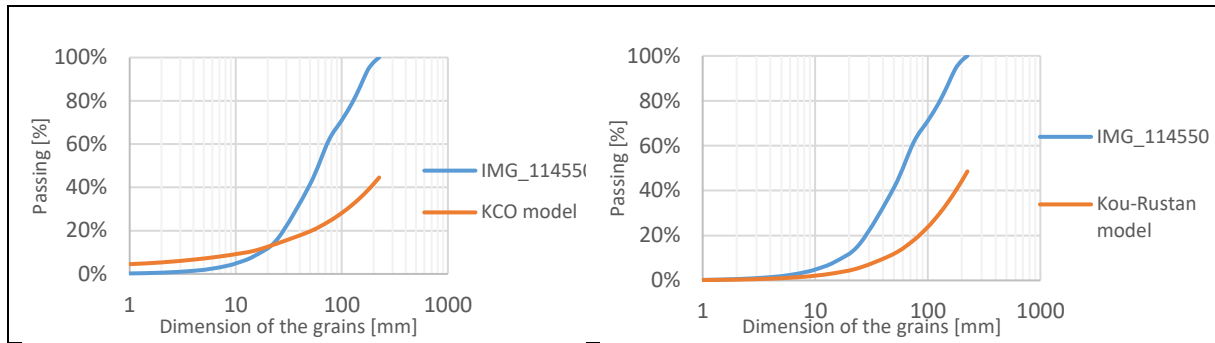


Figure 4. Comparison between the particle size distributions obtained with Split Desktop and with the KCO and Kou-Rustan models.

The SveDeFo model (Figure 5) seems to be the most reliable in terms of comparison with the muck-pile distribution from the quarry; the difference with the previous models is due to the calculation of x_{50} : the average grain size equation includes, in addition to the quality of the rock mass and the type of explosive, the geometry of the pattern. In this case, in both curves, 100% of passing corresponds to dimensions having the same order of magnitude (about 230 mm).

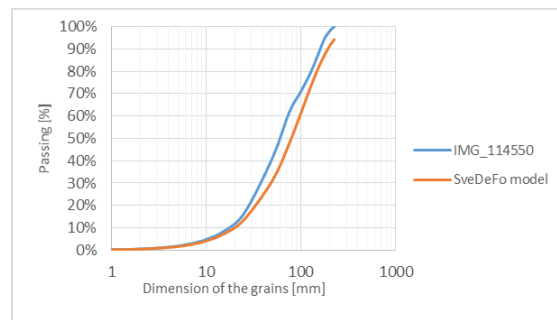


Figure 5. Comparison between the particle size distributions obtained with Split Desktop and the SveDeFo model.

Though the Chung-Katsabani model being very similar to both the Kuz-Ram and Crush-zone models, the trend of the particle size distribution is different (Figure 6). This can be explained by the calculation of the uniformity index (n), where both x_{50} and x_{80} are considered, and by the formulation of the average particle size, which takes into account the geometry of the blast, which vary. This causes both n and x_{50} to be much smaller than in previous models. Although the xP-Frag model is different compared to the previous ones, it provides a good approximation of the curve obtained by Split-desktop for grains larger than about 40 mm. Hence, this model can be recommended in case of coarser fragments.

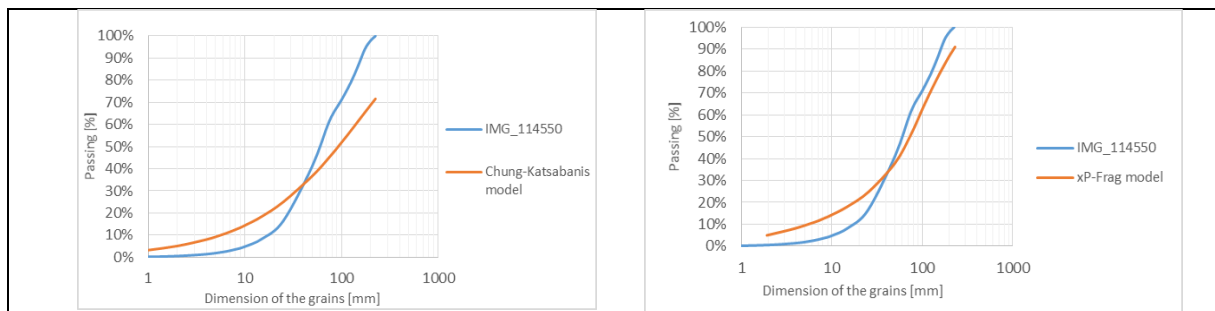


Figure 6. Left: Comparison between the particle size distributions obtained with Split Desktop and with the Chung-Kastabani model and xP-Frag.

4. Conclusions

The purpose of the paper was to provide a comparison between the best known empirical models and the Split-desktop software, to study the grain size distribution from excavation by Drill & Blast. The Split-desktop software made it possible to analyse some images depicting different portions of muck-piles obtained in a limestone quarry. The photographs, however, were not totally characterizing, as the field of the images were sometimes restricted. The analysis showed that the most representative curve is that obtained by applying the SveDeFo model, which is the one that best approximates the distribution depicted by Split-desktop: both curves have the same trend and reach a 100% throughput for grains of the same order of magnitude. The substantial difference between this model and the others is found in the x_{50} formula which, beyond considering the parameters characterizing the explosive and the rock mass, also takes into account the blast geometry. In conclusion, the results obtained by some of the empirical models proposed are comparable with those coming from the software; they can therefore be a good option for the a priori analysis of fragmentation and a valid tool for sizing a blast.

References

- [1] Ouchterlony F 2003 Influence of blasting on the size distribution and properties of muckpile fragments, a state-of-the-art review. MinFo Project P2000-10: Energy Optimisation in Comminution, 114 pp.
- [2] Fourney WL 1993 Mechanisms of rock fragmentation by blasting. Comprehensive Rock Engineering Principles, Practice and Projects, vol 4. Oxford: Pergamon Press, pp. 39–69.
- [3] Katsabanis PD and Omidi O 2015 The effect of delay time on fragmentation distribution through small and medium scale testing and analysis. Fragblast 11. Proc. of the 11th int. symposium on rock fragmentation by blasting, AusIMM, Carlton, Australia, pp. 715-720
- [4] Onederra I, Esen S, Jankovic A 2004 Estimation of fines generated by blasting – applications for the mining and quarrying industries. Mining Technology, 113 (4), pp. 237-247
- [5] Lu W, Leng Z, Chen M, Yan P and Hu Y 2016 A modified model to calculate the size of the crushed zone around a blast-hole. Journal of the Southern African Institute of Mining and Metallurgy, 116, pp. 413-422
- [6] Kuznetsov VM 1973 The mean diameter of the fragments formed by blasting rock. Soviet Mining, 9, pp. 144–148.
- [7] Kanchibotla SS, Valery W and Morrell S 1999 Modelling fines in blast fragmentation and its impact on crushing and grinding. Proceedings of Explo'99—A Conference on Rock Breaking. The Australasian Institute of Mining and Metallurgy, Kalgoorlie, Australia, pp. 137–44.
- [8] Cunningham CVB 2000 The effect of timing precision on control of blasting effects. In R. Holmberg (ed.), Explosives & Blasting Technique: 123–128. Munich–Rotterdam: Balkema.
- [9] Ouchterlony F 2005 The Swebrec© Function: Linking Fragmentation by Blasting and Crushing, Mining Technology (Trans. Instn. Min. Metall. A), 114, pp. A29 – A44.
- [10] Persson PA and Holmberg R 1983 Rock Dynamics. Proc. 5th ISRM Congress, Melbourne, Australia, April 1983, n. ISRM-5CONGRESS-1983-242.
- [11] Ouchterlony F and Sanchidrián JA 2019 A review of development of better prediction equations for blast fragmentation. Journal of Rock Mechanics and Geotechnical Engineering, 11, pp. 1094-1109.
- [12] Shad HIA, Sereshki F, Ataei M and Karamoozian M 2018 Investigation of rock blast fragmentation based on specific explosive energy and in-situ block size. International Journal of Mining and Geoengineering, Volume 52, 1, pp.1-6.
- [13] Chung SH and Katsabanis PD 2010 Fragmentation prediction using improved engineering formulae. Fragblast, 2000(3), pp. 198-207.
- [14] Sanchidrián JA and Ouchterlony F 2017 A Distribution-Free Description of Fragmentation by Blasting Based on Dimensional Analysis. Rock Mechanics and Rock Engineering, 50, pp. 781–806.
- [15] Cunningham CVB 1983 The Kuz–Ram model for prediction of fragmentation from blasting. In R. Holmberg & A Rustan (eds), Proc. First Int. Symposium on Rock Fragmentation by

- Blasting, Luleå, pp. 439–454.
- [16] Vesilind PA 1980 The Rosin-Rammler particle size distribution. *Resource Recovery and Conservation*, 5, 3, pp. 275-277.
- [17] Cunningham CVB 1987 Fragmentation estimations and the Kuz–Ram model – four years on. In W. Fournery (ed.), *Proc. of Second Int. Symposium on Rock Fragmentation by Blasting*, Keystone, Colorado, pp. 475–487.
- [18] Cunningham CVB 2005 The Kuz-Ram fragmentation model – 20 years on. *Brighton Conference Proceedings 2005*, R. Holmberg et al., 005 European Federation of Explosives Engineers, ISBN 0-9550290-0-7, pp. 201-210.
- [19] Sanchidrián JA 2010 *Rock Fragmentation by Blasting*. Proc. 9th Int. Symposium on Rock Fragmentation by Blasting, Sept.2009, Granada, Spain. CRC Press, Sanchidrián Ed.
- [20] Esena S, Onederra I and Bilgin HA 2003 Modelling the size of the crushed zone around a blasthole. *International Journal of Rock Mechanics & Mining Sciences* 40 (2003) pp. 485–495.
- [21] Djordjevic N, Esterle J, Thornton D and La Rosa D 1998 A new approach for prediction of blast induced coal fragmentation. *Proc. of the Mine to Mill 1998 Conference*. The Australasian Institute of Mining and Metallurgy, Brisbane, Australia, pp. 175–81.
- [22] Grundstrom C, Kanchibotla SS, Jankovich A and Thornton D 2001 Blast fragmentation for maximising the sag mill throughput at Porgera Gold Mine. *Proc. of the 27th Annual Conference on Explosives and Blasting Technique*, vol. 1. ISEE, Orlando, FL, USA, pp. 383–99.
- [23] Rustan A, Vutukuri VS. 1983 The influence from specific charge, geometric scale and physical properties of homogeneous rock on fragmentation. *Proc. of the First International Symposium on Rock Fragmentation by Blasting*, Lulea, Sweden, pp. 115–42.
- [24] Szuladzinski G 1993 Response of rock medium to explosive borehole pressure. *Proc. of the Fourth Int. Symposium on Rock Fragmentation by Blasting-Fragblast-4*, Vienna, Austria, pp. 17–23.
- [25] Djordjevic N 1999 Two component model of blast fragmentation. In C.V.B. Cunningham (ed.), *Proc. of Sixth Int. Symposium on Rock Fragmentation by Blasting*, Johannesburg, Symposium Series S21 SAIMM.
- [26] Siddiqui FI, Shah SMA and Behan MY 2009 Measurement of Size Distribution of Blasted Rock Using Digital Image Processing. *JKAU: Eng. Sci.*, Vol. 20, No. 2, pp. 81 – 93.